DOI: 10.13009/EUCASS2023-566
Aerospace Europe Conference 2023 – 10TH EUCASS – 9TH CEAS

Outflow measurements on porous injector elements

Markus Selzer⋆† *and Jonas Peichl*⋆ *and Ivens Daniel Hoffmann*△ *and Dmitry Suslov* △
⋆*German Aerospace Center, Institute of Structures and Design*
70569 STUTTGART, Germany
Markus.Selzer@dlr.de · Jonas.Peichl@dlr.de
△*Stuttgart University, Institute of Space Systems*
70569 STUTTGART, Germany
Ivens.Hoffmann@dlr.de
△*German Aerospace Center, Institute of Space Propulsion*
74219 LAMPOLDSHAUSEN, Germany
Dmitry.Suslov@dlr.de
†Corresponding author

Abstract

In this report, the outflow distribution on a porous injector element is measured on the pore level using dynamic pressure measurements. The results are used to link features in the outflow distribution to the characteristics of the specific porous material. Furthermore, the flow direction of the individual outflow jets is investigated and finally the evolution of the flow field downstream of the injector element is analysed. The results provide further understanding of the flow field created by the porous injector element, hinting also at possible optimizations of this technology.

1. Introduction

Shear-Coaxial injectors represent the state of the art for injectors used in gas-/liquid-fueled rocket engines. When carefully designed, very high mixing efficiencies are possible. On the downside, these high mixing efficiencies are only possible within a narrow operating regime and require precise manufacturing. This limits throttling capability and results in high manufacturing cost.[7] In contrast, porous injection concepts maintain high mixing efficiency over a wide throttling range.[2] Additionally, the efficiency is not as sensitive to manufacturing tolerances, resulting in easier manufacturing. Finally, the pressure loss over the injector can be minimized by the design of the porous media. Although atomization mechanisms for porous injectors have been developed by Deeken et al.,[3] the detailed outflow distribution of the propellant from the porous surface is up to now not known in detail. Therefore, in this work the outflow distribution of a porous face plate of a small injector element is characterized. For this, the AORTA (Advanced Outflow Research facility for Transpiration Applications) test bench developed at the DLR Institute of Structures and Design is used. The test bench enables the characterization of porous materials regarding their permeability and outflow distribution. Therefore, porous samples or components can be perfused by gaseous nitrogen with mass flows from 0.02 g/s to 12 g/s at pressures up to 15 bar. The mass flow rates, pressures and temperatures are recorded. With these measurements, the permeability can be determined, describing the pressure loss of the fluid flow through the porous medium. This permeability is usually expressed by the well-known Darcy-Forchheimer equation. Additionally, the outflow distribution of the porous material can be characterized by measuring dynamic pressures via pitot tubes mounted on linear axes. To measure the outflow distribution, the pitot tube is moved over the sample and stationary pressure measurements are automatically done. This allows for an automated, detailed measurement of the outflow characteristics as will be shown in the current report.

2. Description of test setup

The injector element examined in this report was provided by the DLR Institute of Space Propulsion in Lampoldshausen. It consists of several layers of stainless steel wire mesh, as seen in figure 1 on the left, taken from.[4] Each layer consists of 64 warp threads and 12 weft threads per inch. The thread diameters are approximately 0.4 mm (warp) and 0.6 mm (weft). Starting with this mesh, several layers are sintered to get a permeable plate. From this plate the porous injector face plates are manufactured. The porous face plate of the element as shown in the middle of figure 1 has an

DOI: 10.13009/EUCASS2023-566

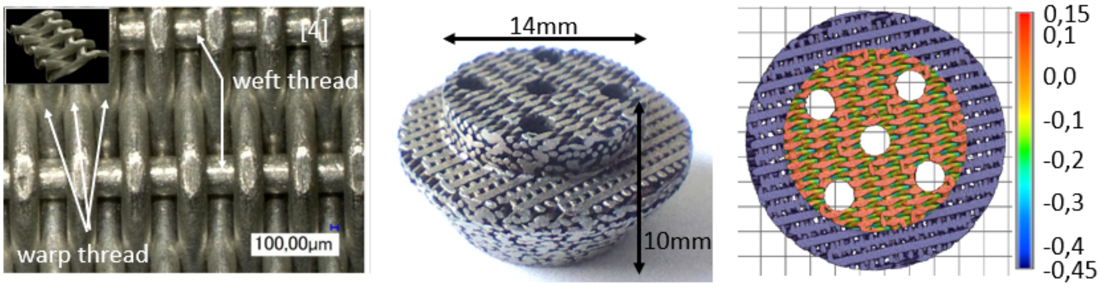

Figure 1: Rigimesh injector element characterized in this study

outflow diameter of 14 mm and a thickness of 10 mm. Additionally, 5 holes with a diameter of 2.4 mm are drilled in the plate. Through these holes, tubes for injecting the oxidiser are installed, but are not used in the present study. These tubes are simply passed through the holes in the face plate without any additional sealant to ensure tightness. In the height map on the right of figure 1 it can be seen, that the outflow area is not an even plane, but shows the typical mesh pattern with peak to peak distances of approximately 0.6 mm. Also, some irregularities in the mesh pattern can be seen, where two layers of mesh have been cut during machining to get the desired thickness of the face plate.

This injector element was installed in a sample holder and connected to the AORTA facility. Here, a well defined nitrogen gas flow can be applied to the sample and the outflow distribution can be measured. For the results presented here, the mass flow was always kept at 0.39 g/s. During the measurement a pitot tube is moved by high precision linear units (positional accuracy $< 10\,\mu m$) driven by step motors. The sensor is moved in a meander pattern over the sample and the control software automatically acquires stationary dynamic pressure values for each point as the mean value over 20 measurements. For the outflow measurements, two different pitot tubes with inner diameters of 0.8 mm and 0.3 mm have been used, both connected to a pressure transducer PTSXR from Airflow Lufttechnik GmbH with a maximum pressure of 1000Pa. The sensor inherited uncertainty for the measurement chain amounts to 7 Pa. The mass flow is measured by a M14 Coriolis with an uncertainty below 0.5 %.

Another important parameter for the measurements is the distance from the pitot tube to the sample. This distance is determined by moving the pitot tube in increments of 1/100 mm to the sample until a consistent electrical contact can be measured. To take into account the roughness of the sample, a small metallic plate with a thickness of 1 mm is placed on the sample for these measurements. The repeatability of this measurement is typically ± 1/100 mm. Also, with measurements of 4 points on the sample plane, the sample plane is also aligned to the x-y-plane of the sensor, with deviations in height of these points below 7/100 mm during the shown measurements.

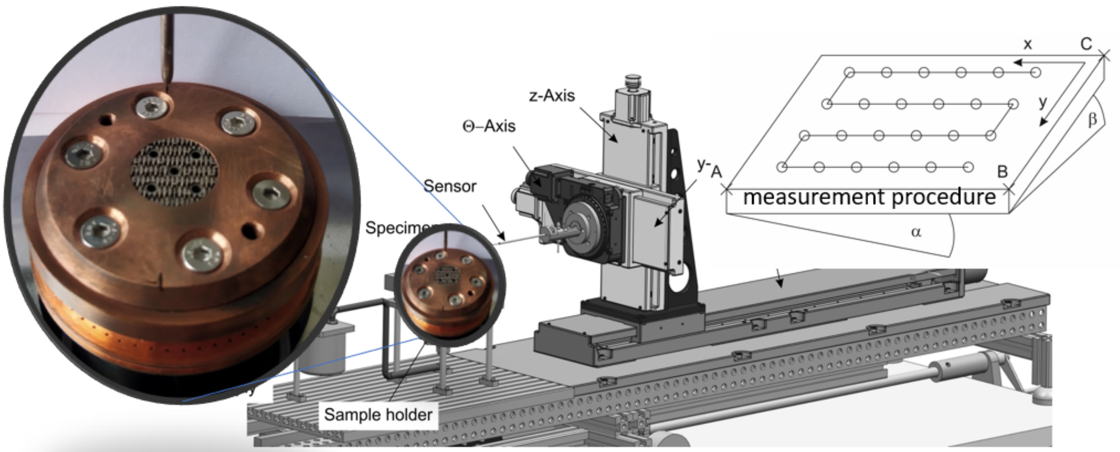

Figure 2: Test setup and measurement procedure

DOI: 10.13009/EUCASS2023-566

3. Measurement results

3.1 Outflow distribution measurements

Often the flow through a porous medium is assumed to be homogenous and an average velocity is used to describe the porous flow. But on a pore scale, the flow is made up of fluid jets flowing out of the pores and regions with no outflow between the pores. Depending on the size of the pitot tube compared to the pore size and distribution, it is obvious, that the measured distribution already contains some sort of averaging. This principle is shown in figure 3 on the left side. Besides this averaging, additional errors are induced by the pitot tube disturbing the flow. Thus, the absolute measured pressure values are distorted and should not be taken as the true values. This was already described in.[8–10] Nonetheless, the measurements are able to differentiate between regions with flow, e.g. pores, and regions without flow and higher pressure values correlate to higher velocities and thus higher mass flow. In the past, transpiration cooling experiments showed, that these distributions are consistent with the cooling efficiencies measured. Interpreted as relative distributions they were also used as boundary conditions in numerical simulations.[6] The simulations showed good agreement with the measurements, a good indication that these relative distribution are valid.

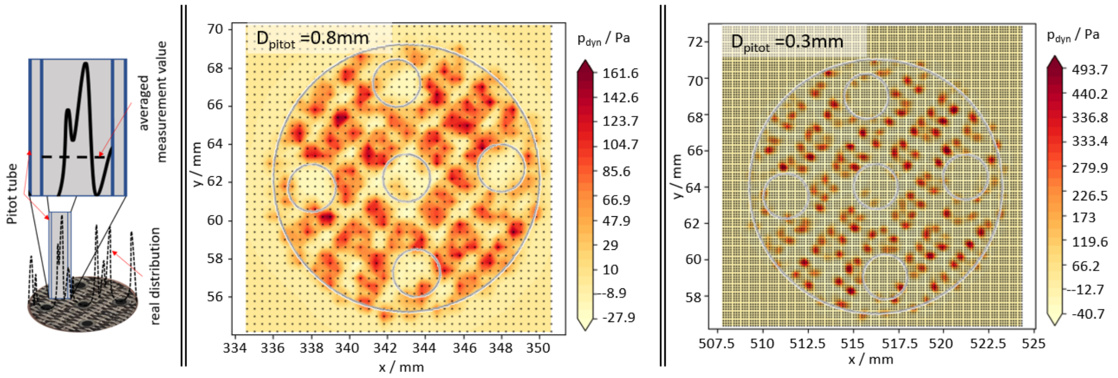

Figure 3: Outflow measurements with 0.8 mm and 0.3 mm Pitot tube, distance 0.3 mm

For the outflow measurements shown in this report, two different pitot tubes with inner diameters of 0.8 mm and 0.3 mm have been used. The step size between two measurement points was chosen as half of this diameter. Consequently, the measurement density is approximately 8.5 and 50 pts/cm^2 respectively. The time to measure the whole injector element scales accordingly. In practice, while two to three measurements per day are possible with the larger pitot tube, measurements with the small pitot tube take approx. 5 times longer. Figure 3 shows the results of such measurements as a contourplot of the measured dynamic pressures on the x-y-plane. In the middle the 0.8 mm and on the right the 0.3 mm pitot tube was used. The black dots in the plots represent the stationary measurement points. For better orientation, the outline of the sample is also given in the plot. The measurements with a smaller pitot tube show the distribution in higher resolution, whereas the 0.8 mm pitot tube already provides more averaged results. This also results in the absolute measured pressures with the smaller pitot tube being higher. The explanation for this effect, is the smaller averaging area of the smaller pitot tube, thus individual jets of the outflow are represented better. Also notable are the negative pressures that can be seen especially at the edge of the injector element and above the injection tubes, indicating recirculation and inflow of adjacent ambient air. As the objective of the measurements in this report is to solely characterize the outflow distribution, these flow phenomena are ignored in later plots, e.g. negative pressures are set to zero.

3.1.1 General outflow characteristics

To further discuss the measured outflow distribution, Figure 4 shows a measured outflow distribution compared to the heightmap of the same sample. This measurement was conducted with the 0.3 mm pitot tube at a distance of 0.3 mm. The distribution is very regular, but also coarse with nearly all the jets located on straight lines. On the right in figure 4, a binary map of the measured outflow jets is superimposed with the height map. It can be seen, that the outflow jets are all located next to the weft thread, more specifically where the warp thread runs under the weft thread. Also visible in the outflow distribution is a chequered pattern, with each region including six neighbouring jets as indicated in detail A. This can be explained by the layup of the meshes, where each mesh is rotated by 90° compared to the previous mesh. Thus it is shown, that the last two layers influence the outflow distribution. Interestingly, despite not

DOI: 10.13009/EUCASS2023-566

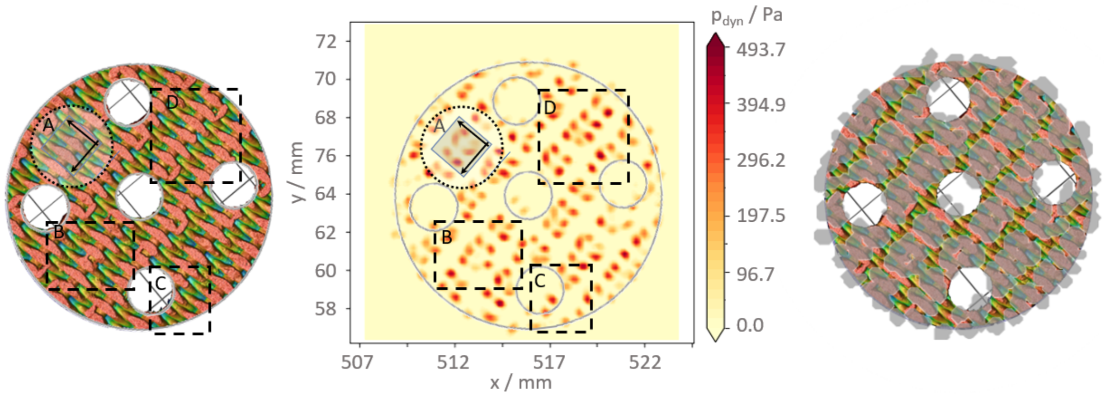

Figure 4: General outflow characteristics (D_{pitot}=0.3 mm, distance 0.3mm)

using any sealant between porous medium and the holes for the oxidiser tubes or at the edges of the injector element, no relevant leakage could be detected. Careful machining is enough to prevent any leakage, which simplifies the injection concept considerably. Finally, the absolute values show some variation, with higher outflow in the region of detail D. The reason is unknown, but it is assumed that small irregularities in the individual meshes and in the layup cause these inhomogeneities. The influence of these inhomogeneities on the flow field further downstream of the injector element is shown in section 3.1.2.

The measurements also allow for more detailed analyses of irregularities in the outflow distribution. As examples, figure 5 shows three regions on the sample. In detail B, the measurements show a jet that deviates from the straight line of jets. For this jet, the height map shows a blocked pore, that deflects the jet from the straight line.
Detail C shows the measurements of a jet at the location of the oxidiser tubes, where no outflow is expected. When looking at the height map, one can see that the pore of this jet is located exactly at the oxidiser tube hole. The resulting jet is then diverted in the direction of the hole.
In detail D, the height map shows remains of the adjacent mesh, that was removed during machining of the sample. But in contrast to region A, these irregularities do not block the pore and thus the jets are not influenced.

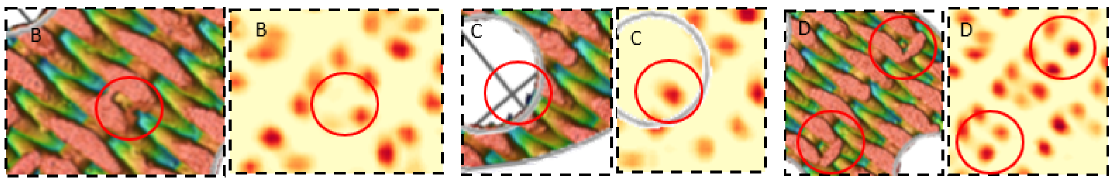

Figure 5: Details of outflow distribution

Using these results, it is imaginable to develop an enhanced porous face plate material. For example a finer mesh will also result in a finer outflow distribution. Additionally, it is possible to identify the influence of different processing steps in the manufacturing of the porous material on the outflow variations and patterns shown here.

3.1.2 Mixing of jets with increasing distance

According to the theory of turbulent jets,[1] with increasing distance to the pore, the flow profile of the individual jet will widen in radial direction, while the peak velocity will decrease. Eventually the individual jets will mix and the flow will become more homogenous. For the injection of fuel in a combustion chamber, this mixing should happen as fast and efficient as possible. In this chapter, this evolution of the outflow distribution with further distance to the sample is investigated by repeating the measurement at different distances to the injector element.

Figure 6 shows the flow distribution at distances from 0.3 mm up to 6.0 mm. All measurements were done with the small pitot tube and a constant mass flow. Unfortunately, after the 2 mm measurement the injector element was moved, resulting in a rotation of the distribution by approximately 40°, but the patterns in the distribution are still clearly visible. In general, with increasing distance the absolute measured pressures decrease. This is in accordance to the theory of free jets, where the velocity of the flow decreases with increasing distance. It can be seen, that on the injector element scale, the measurements show no relevant widening of the flow, with the vast majority of the massflow still within the bounds of the injector element. But on the pore scale, the widening of the individual jets is clearly

DOI: 10.13009/EUCASS2023-566

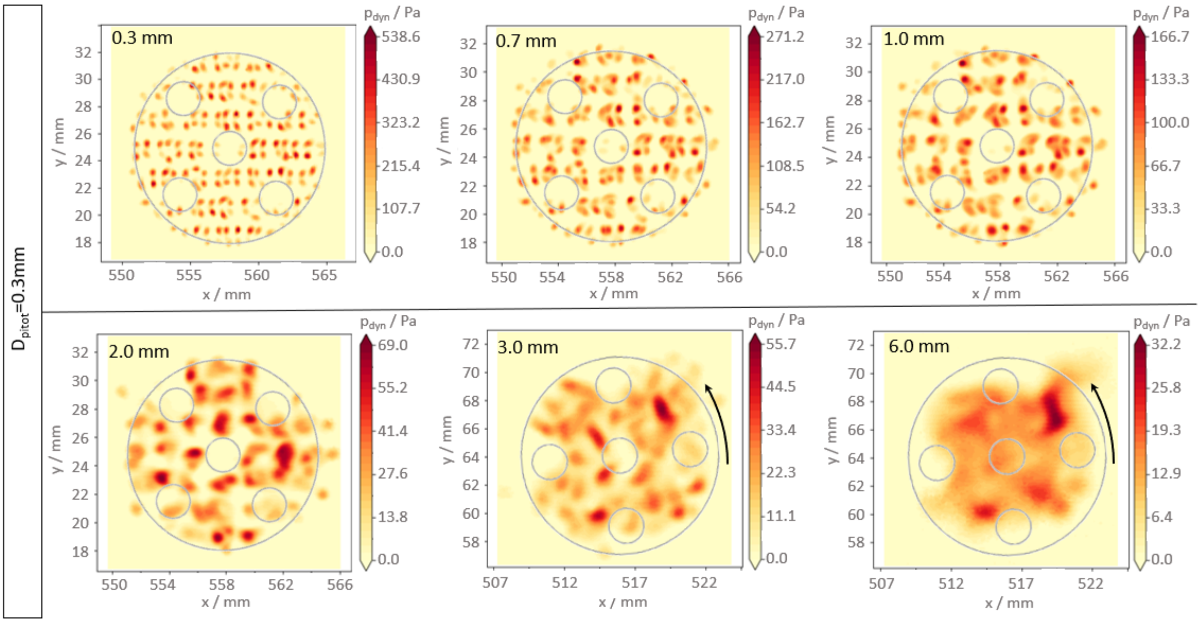

Figure 6: Mixing of jets from 0.3 mm to 6.0 mm distance

visible. At 0.7 mm, the six jets in the already mentioned groups start to mix. At 2.0 mm distance, this process is mostly finished. The distribution is now made up of the blended jets from these groups. At 3 mm distance, these blended jets start to mix again until at 6 mm the flow distribution shows 4 peaks, divided by the oxidiser injection tubes. The highest peak in the distribution is in the region of detail D, given in figure 5, where also the highest pressures for the individual jets could be measured. Thus, these inhomogeneities have an influence even far downstream of the sample.

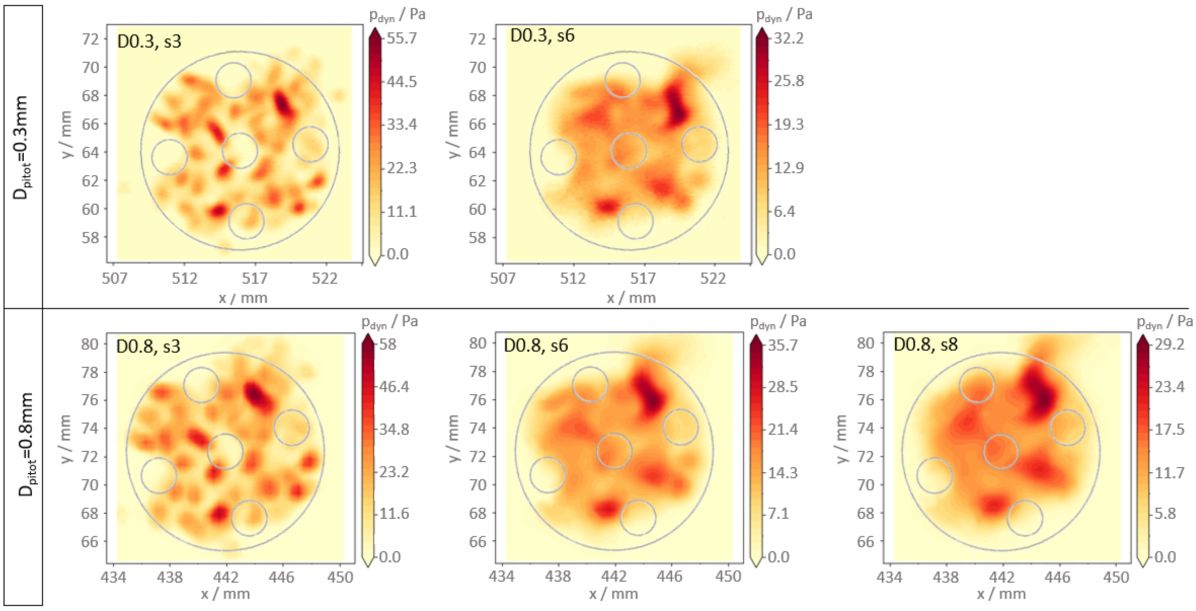

Figure 7: Comparison pitot tube diameter from 3.0 mm to 8.0 mm distance

It was shown before (see Chapter 3.1), that at small distances the measured distribution and pressure values are quite different. This is explained by the averaging of the flow field over the pitot tube, the size of the pitot tube defining the resolution of the results. But with further homogenization of the flow field downstream of the injector element, this effect will vanish. Concluding the investigation on the flow field development, Figure 7 shows measurements with the two pitot tubes at the same distances. Indeed, the measurements show very comparable results in distribution and absolute values starting at a distance of 3 mm. Further downstream, the larger pitot tube is sufficient for measurement,

DOI: 10.13009/EUCASS2023-566

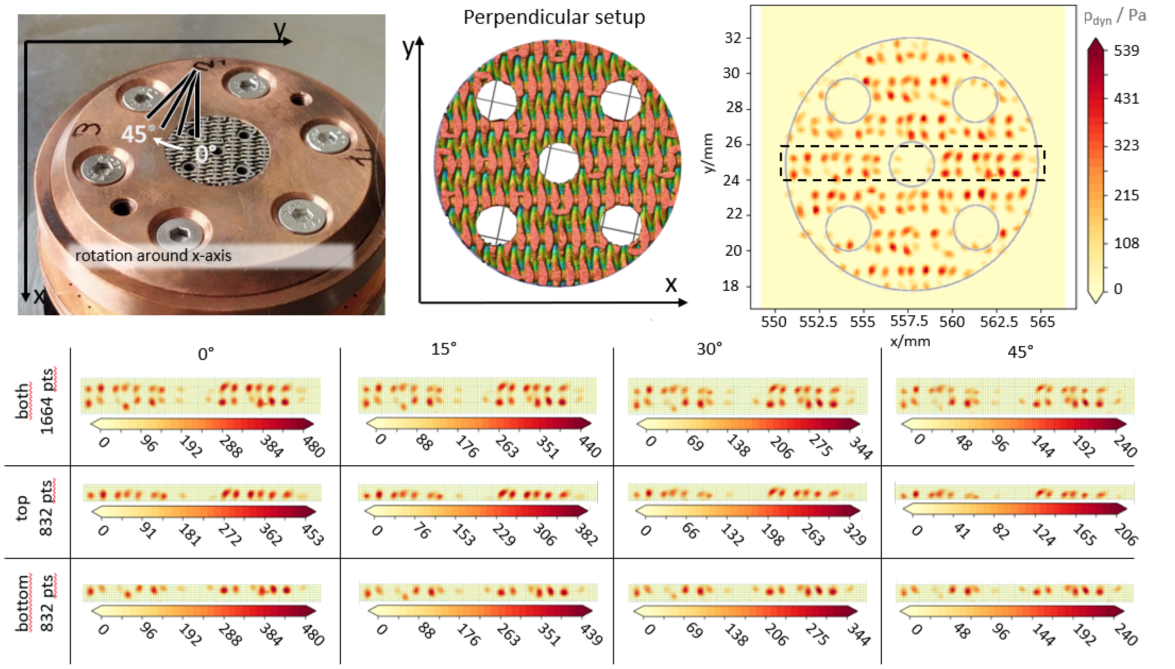

Figure 8: Perpendicular setup and details

yielding big savings in measurement time.

3.1.3 Measurements with inclined Pitot tube

Given the structure of the material used, it is assumed, that the flow is not necessarily always normal to the surface. The shape of the jets in the contour plots, also seem to suggest an inclined direction of the jets. In the following chapter these assumptions are further investigated.

As pitot tubes are sensitive to the direction of the flow, they can be used to measure the direction of macroscopic flows: the pitot tube is aligned to the flow, when the maximum velocity is measured. For real porous materials, the individual jets will vary from each other in direction and intensity. Therefore, of interest for the macroscopic flow is not every individual jet, but more general trends. Dittert et al. showed in,[5] that it is possible to determine such general trends by analysing mean pressures over representative areas of the material. When defining these areas, it has to be considered that by averaging over a lot of jets, the direction of these jets is also averaged. Thus opposite flow directions in the area cannot not be detected. The averaging also naturally leads to much smaller absolute pressures, as most of the surface shows no or very little through flow. All measurements in this section are conducted with the 0.3 mm pitot tube at a distance of 0.3 mm. With the given test bench, the pitot tube can only be rotated about the x-axis and only flow inclined in the y-direction can be investigated. For investigations involving different outflow directions, the injector element has to be aligned accordingly. This way two positions were investigated in this study, each testing one assumption. First it is assumed, that the weft thread deflects the pore flow normal to the weft thread direction. The second assumption is based on the measured distributions, where the shape of the individual jets suggest an inclination of the jets in 45° to the weft thread.

To test the first assumption, a perpendicular setup, as shown in figure 8, has been investigated. The alignment of the injector element to the x-y-plane of the test bench as well as the angle of the pitot tube is depicted in the first row of figure 8. The injector element was measured with pitot tube angles of 0°, 15°, 30° and 45°. On the right in the first row, the contour plot of the whole injector element is given for the 0°-measurement. As representative for the assumed deflection by the weft thread, the jets around the center weft thread are shown in more detail. Each investigated area in a row contains the same number of measurement points in x- and y-direction. The different rows show first both sides of the flow around the weft thread together (both). As it is expected, that the jets on both sides of the weft thread would be deflected in opposite directions, also the jets above (top) and below (bottom) the weft thread are shown separately. If the jets on the top side are deflected in the direction of the pitot tube, the values should increase for that row of jets, whereas the values for the bottom row should decrease.

The measurements show, in contrast to these assumptions, that while the general pattern stays very comparable for all rotation angles, the absolute measured pressures are consistently decreasing with increasing measurement angle

DOI: 10.13009/EUCASS2023-566

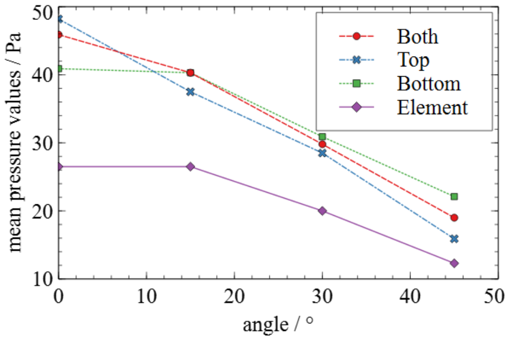

Figure 9: Mean pressures for perpendicular setup

for all areas.

This is also confirmed in figure 9, where the mean pressures over the depicted areas are shown in dependence on the measurement angle. Added is also a line with the mean pressure values over the whole injector element. The absolute values are smaller, because the measurement points outside of the injector element are included. All curves show the same trend, which leads to the conclusion, that no relevant deflection of the flow by the weft thread could be detected, at least for the investigated angles.

To test the second assumption, the injector element was rotated by 45 degrees, as shown in figure 10, and the measurement was repeated. Again, the measurements were conducted with the 0.3 mm pitot tube at a disctance of 0.3 mm, this time for pitot tube angles of 0°, 10°, 20° and 30°. A representative area of the surface was chosen for further analysis as indicated in figure 10.

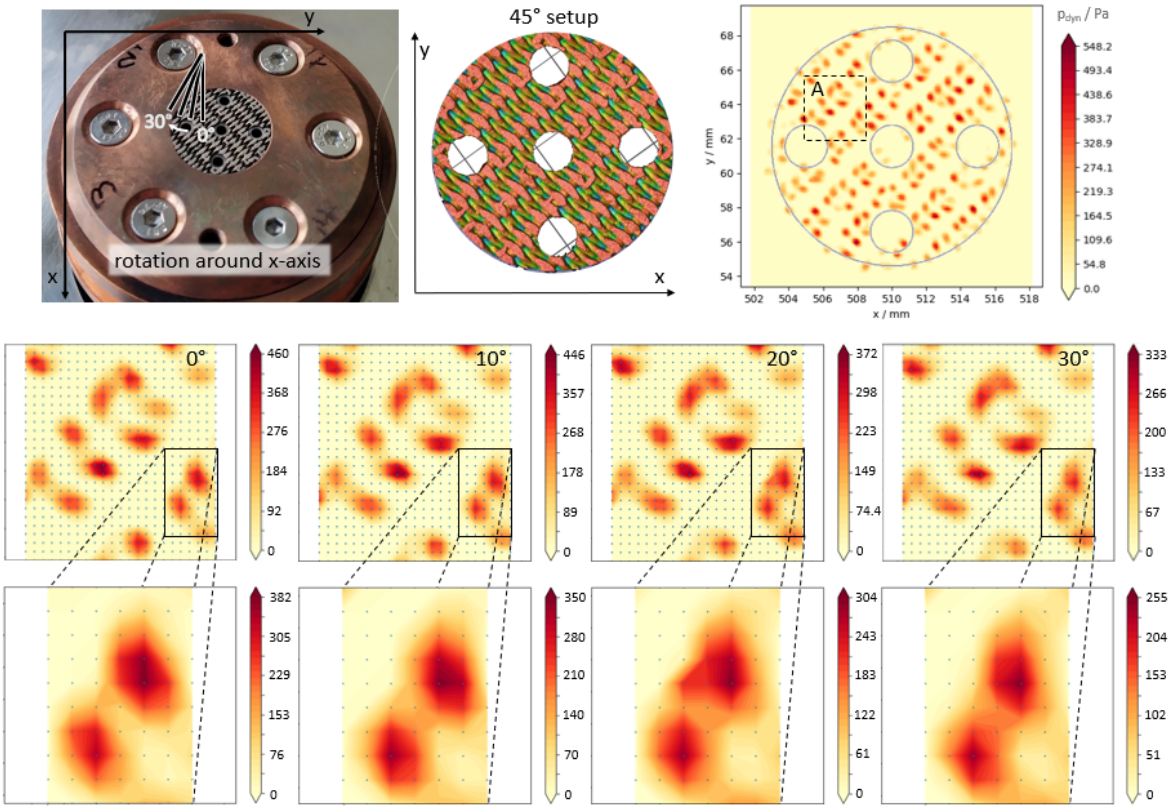

Figure 10: 45° setup and details

The patterns in the contour plots again barely change with the pitot tube angle, but the measured pressures decrease. In the last row of figure 10 two jets, seemingly inclined in y-direction are shown. Despite the shape of the jets, the measured values again decrease with further rotation. Figure 11 shows the mean values over the respective

DOI: 10.13009/EUCASS2023-566

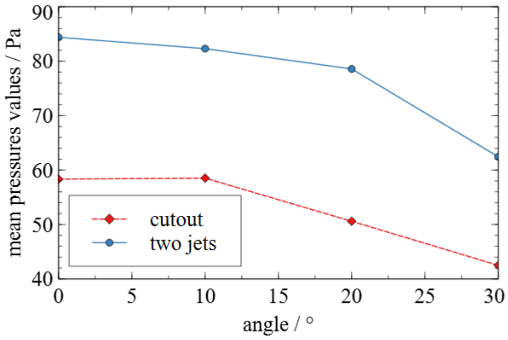

Figure 11: Mean pressures for 45° setup

areas, again showing the decreasing trend in pressures with increasing rotation angle. So again, the measurement results do not support the assumption for the investigated angles for angles between 10° and 30°.

4. Conclusion and outlook

The outflow distribution on a porous injector element is measured on the pore level. The porous material is based on sintered wire meshs. The measurements show a very regular outflow distribution, with flow only where the warp thread runs under the weft thread. With the measurements it could be shown, that not only the last mesh in the porous material influences the outflow distribution, but also the layer below has a direct impact. The weft thread from this layer blocks the flow, which results in a chequered outflow pattern with 6 jets grouped together. With measurements on the flow field downstream of the surface, the further evolution of the flow is investigated. At 2 mm downstream, the group of six jets is blended into one single, larger jet. Between 2 mm and 6 mm these bigger jets blend together and form a more continuos flow field. At this distance, the impact of the size and distribution of the oxidiser tubes is clearly visible, with peaks in the flow field between these tubes. Also some inhomogeneities in the outflow rate of the individual pores still impact the homogeneity at this distance. An assumed non-normal outflow of the porous flow could not be found for two possible outflow directions and with inclination angles of the pitot tube between 10° and 45°.

The results provide a deeper understanding of the flow field created by the porous injector element, hinting also at possible optimizations of this technology. From the results it is concluded, that the use of smaller threads in the wire mesh should provide a finer distribution of the jets. Measuring the small inhomogeneities in the outflow pressures could also be used to optimize the manufacturing process of the porous material to provide a more homogenous flow over the complete surface. The presented measurements also provide valuable knowledge of the flow evolution downstream of the face plate. The size and distribution of the oxidiser tubes is identified as the main impact on the downstream flow distribution.

The investigations so far were limited to one porous material and flow was restricted to the porous face plate. In the future it will be interesting to also include flow through the oxidiser tubes. Also, measurements on a sintered bronze powder based material, also previously investigated for the porous injector technology, are planned. Combining these investigations with results on combustion test benches regarding combustion quality, promise to enable a more targeted optimization of this technology.

References

[1] G. N. Abramovich and L. Schindel. *The theory of turbulent jet*. MIT-Press, Cambridge, Massachusetts, 1963.

[2] J. Deeken, D. Suslov, O.J. Haidn, and S. Schlechtriem. Combustion efficiency sensitivity studies of the api injector concept. 49th Aerospace Sciences Meeting including the New Horizons Forum and Aerospace Exposition, 2011.

[3] J. C. Deeken, D. I. Suslov, M. Oschwald, S. Schlechtriem, and O. J. Haidn. Propellant atomization for porous injectors. *Journal of Propulsion and Power*, 35(6):1116–1126, 2019.

[4] Jan C. Deeken. *Experimentelle Untersuchungen zu neuartigen, porösen Injektoren für den Einsatz in kryogenen Hochdruck-Raketenantrieben*. Dissertation, Universität Stuttgart, 2014.

[5] Christian Dittert, Markus Selzer, and Hannah Böhrk. Flowfield and pressure decay analysis of porous cones. *AIAA Journal*, 55(3):874–882, 2017.

DOI: 10.13009/EUCASS2023-566

[6] V. König, M. Rom, S. Müller, M. Selzer, S. Schweikert, and J. Von Wolfersdorf. Numerical and experimental investigation of transpiration cooling with carbon/carbon characteristic outflow distributions. *Journal of Thermophysics and Heat Transfer*, 33(2):449–461, 2019.

[7] J. Lux, D. Suslov, and O.J. Haidn. On porous liquid propellant rocket engine injectors. *Aerospace Science and Technology*, 12, 2008.

[8] M. Selzer, H. Hald, S. Schweikert, and J. von Wolfersdorf. Measurements of surface exhalation characteristics of porous fibre reinforced composites. 4th International Conference on Porous Media and its Applications in Science and Engineering, 2012.

[9] M. Selzer, S. Schweikert, H. Böhrk andH. Hald, and J. von Wolfersdorf. Comprehensive c/c sample characterizations for transpiration cooling applications. Technical report, Annual Report, SFB Transregio 40, 2016.

[10] M. Selzer, S. Schweikert, H. Hald, and J. von Wolfersdorf. Throughflow characteristics of c/c. Technical report, Annual Report, SFB Transregio 40, 2014.